

Computerized electrocardiogram data transformation enables effective algorithmic differentiation of wide QRS complex tachycardias

Anthony H. Kashou MD¹ | Sarah LoCoco MD² | Preet A. Shaikh MBBS³ |
Bhavesh B. Katbamna MD² | Ojasav Sehrawat MBBS¹ | Daniel H. Cooper MD³ |
Sandeep S. Sodhi MD, MBA³ | Phillip S. Cuculich MD³ | Marye J. Gleva MD³ |
Elena Deych MS⁴ | Ruiwen Zhou PhD⁴ | Lei Liu PhD⁴ | Abhishek J. Deshmukh MBBS¹ |
Samuel J. Asirvatham MD¹ | Peter A. Noseworthy MD¹ |
Christopher V. DeSimone MD, PhD¹ | Adam M. May MD³ 

¹Department of Cardiovascular Medicine, Mayo Clinic, Minnesota, Rochester, USA

²Department of Medicine, Washington University School of Medicine, Missouri, St. Louis, USA

³Department of Medicine, Division of Cardiovascular Diseases, Washington University School of Medicine, Missouri, St. Louis, USA

⁴Division of Biostatistics, Washington University School of Medicine, Missouri, St. Louis, USA

Correspondence

Adam M. May, 660 S. Euclid Ave, CB 8086, St. Louis, MO 63110, USA.
Email: may.adam@wustl.edu

Abstract

Background: Accurate automated wide QRS complex tachycardia (WCT) differentiation into ventricular tachycardia (VT) and supraventricular wide complex tachycardia (SWCT) can be accomplished using calculations derived from computerized electrocardiogram (ECG) data of paired WCT and baseline ECGs.

Objective: Develop and trial novel WCT differentiation approaches for patients with and without a corresponding baseline ECG.

Methods: We developed and trialed WCT differentiation models comprised of novel and previously described parameters derived from WCT and baseline ECG data. In Part 1, a derivation cohort was used to evaluate five different classification models: logistic regression (LR), artificial neural network (ANN), Random Forests [RF], support vector machine (SVM), and ensemble learning (EL). In Part 2, a separate validation cohort was used to prospectively evaluate the performance of two LR models using parameters generated from the WCT ECG alone (Solo Model) and paired WCT and baseline ECGs (Paired Model).

Results: Of the 421 patients of the derivation cohort (Part 1), a favorable area under the receiver operating characteristic curve (AUC) by all modeling subtypes: LR (0.96), ANN (0.96), RF (0.96), SVM (0.96), and EL (0.97). Of the 235 patients of the validation cohort (Part 2), the Solo Model and Paired Model achieved a favorable AUC for 103 patients with (Solo Model 0.87; Paired Model 0.95) and 132 patients without (Solo Model 0.84; Paired Model 0.95) a corroborating electrophysiology procedure or intracardiac device recording.

This is an open access article under the terms of the [Creative Commons Attribution-NonCommercial](https://creativecommons.org/licenses/by-nc/4.0/) License, which permits use, distribution and reproduction in any medium, provided the original work is properly cited and is not used for commercial purposes.

© 2022 The Authors. *Annals of Noninvasive Electrocardiology* published by Wiley Periodicals LLC.

Conclusion: Accurate WCT differentiation may be accomplished using computerized data of (i) the WCT ECG alone and (ii) paired WCT and baseline ECGs.

KEYWORDS

ventricular tachycardia/fibrillation <basic, non-invasive techniques—
electrocardiography <clinical

1 | INTRODUCTION

Accurate and timely wide QRS complex tachycardia (WCT) differentiation into ventricular tachycardia (VT) and supraventricular wide QRS tachycardia (SWCT) by way of 12-lead electrocardiogram (ECG) interpretation is a critical responsibility for frontline healthcare providers. However, despite its undeniable clinical importance, the successful distinction of VT from SWCT continues to be a difficult task in clinical practice, especially for clinicians lacking sufficient ECG interpretation expertise or a practiced proficiency using traditional ECG interpretation methods (Baxi et al., 2012; Isehour et al., 2000; May et al., 2018). Inopportune occasions that call attention to this limitation are commonplace, especially among clinicians who regularly encounter patients with VT or SWCT within demanding and high-stress clinical environments (e.g., emergency departments and intensive care units).

Although numerous WCT differentiation criteria and algorithms are readily available for clinical use (Akhtar et al., 1988; Brugada et al., 1991; Chen et al., 2019; Griffith et al., 1994; Jastrzebski et al., 2017; Kindwall et al., 1988; Lau et al., 2000; Marriott, 1970; Moccetti et al., 2022; Pachon et al., 2019; Pava et al., 2010; Sandler & Marriott, 1965; Vereckei et al., 2008; Wellens et al., 1978), each universally possesses inherent and inescapable limitations relating to their manual application. In genuine “real-life” clinical circumstances, frontline clinicians must do the following to accurately differentiate WCTs with a 12-lead ECG:

- (i) acquire and then visually inspect a properly recorded and well-timed 12-lead ECG that sufficiently “captures” the WCT event,
- (ii) summon forth or precisely recall one or more of the available WCT differentiation criteria or algorithms, and
- (iii) sedulously implement the chosen WCT differentiation method(s) without error, even while under duress.

As such, accurate and timely WCT differentiation may be upended by the practical limitations of manual methods, and serious clinical mistakes may ensue despite clinicians' well-intentioned attempts to differentiate WCTs accurately. On occasions where frontline clinicians arrive at a delayed or inaccurate VT or SWCT diagnosis, WCT patients may be unintentionally exposed to harmful medical treatments, missed therapeutic opportunities or unsafe management decisions.

Given the inherent challenges associated with manually operated WCT differentiation methods, we created automated solutions to distinguish VT and SWCT, including the WCT Formula (2019) (May et al., 2019a), VT Prediction Model (2020) (May et al., 2020), WCT Formula II (2020) (Kashou, DeSimone, Deshmukh, et al., 2020), and VCG Model (2021) (Kashou et al., 2021). The fundamental

characteristic of each proposed method is the integration of novel mathematically formulated parameters (e.g., frontal percent amplitude change [PAC] [%] or horizontal percent time-voltage area change [PTVAC] [%]), directly derived from computerized ECG measurement data, into an automatic binary classification model. For each method (Kashou et al., 2021; Kashou, DeSimone, Deshmukh, et al., 2020; May et al., 2019a, 2020), we found that automated WCT differentiation models can provide an effective means to differentiate WCTs accurately. However, given that each automated WCT differentiation method requires the simultaneous analysis of paired WCT and baseline ECG data, they cannot be immediately applied to patients without a previously recorded and archived baseline ECG.

Our objective was to develop and evaluate novel WCT differentiation approaches applicable to patients *with* and *without* a baseline ECG. Central to this analysis is the introduction of a novel parameter (i.e., percent monophasic time-voltage area [PMonoTVA] [%]) that may be derived from computerized ECG measurements present on the WCT ECG alone. Distinctively, PMonoTVA may be incorporated into novel WCT differentiation models applicable to any WCT patient, whether they present with or without a corresponding baseline ECG.

2 | METHODS

2.1 | Study design

In a two-part investigation we developed, trialed, and compared novel WCT differentiation models comprised of novel (i.e., PMonoTVA) and previously described WCT differentiation parameters derived from WCT and baseline ECG data. In Part 1, a derivation cohort of paired WCT and baseline ECGs were examined to generate and evaluate high-performing logistic regression (LR) and machine learning (ML) models designed to automatically distinguish WCTs into VT and SWCT. In Part 2, two LR models (i.e., Solo Model and Paired Model) were prospectively evaluated against a separate validation cohort of paired WCT and baseline ECGs.

2.2 | ECG selection

All paired WCT and baseline ECGs were recorded from patients who presented in real-life clinical settings. ECGs were standard 12-lead recordings (paper speed: 25 mm/s and voltage calibration: 10 mm/mV) accessed from data archives provided by a proprietary ECG interpretation software system (MUSE [GE Healthcare]). WCTs were required to satisfy standard WCT criteria (QRS duration ≥ 120 ms

and ventricular rate ≥ 100 beats per minute) and possess an official ECG interpretation of (i) "VT," (ii) "supraventricular tachycardia," or (iii) "wide complex tachycardia." Baseline ECGs were defined as the first non-WCT rhythm recorded *after* the WCT event.

Polymorphic WCTs and WCTs demonstrating grossly irregular atrioventricular conduction (e.g., atrial fibrillation or atrial flutter with variable atrioventricular block) were excluded, and ECGs demonstrating truncated WCTs (e.g., brief run of non-sustained VT) occurring within a dominant baseline heart rhythm (e.g., normal sinus rhythm) were not evaluated. If a WCT did not have a baseline ECG or definitive clinical diagnosis established by the patient's overseeing physician, it was excluded from further analysis. Among patients having multiple WCT events, the surplus of WCT ECGs occurring after the first WCT event were excluded (i.e., a single WCT and baseline ECG pair was evaluated per patient).

2.3 | Study cohorts

2.3.1 | Derivation cohort

The derivation cohort comprised 421 consecutive patients with paired WCT and baseline ECGs acquired at the Mayo Clinic Rochester or Mayo Clinic Health System of South Eastern Minnesota (September 1, 2011 through November 30, 2016). The ECG selection processes and clinical characteristics of this patient cohort are thoroughly described

in previous reports (Kashou, DeSimone, Hodge, et al., 2020; May et al., 2019a, 2019b, 2020). The Mayo Clinic Institutional Review Board approved patient data acquisition and analysis.

2.3.2 | Validation cohort

The validation cohort comprised 235 consecutive patients with paired WCT and baseline ECGs obtained at Barnes-Jewish Hospital in St. Louis (January 1st, 2012 through December 31st, 2014). **Figure 1** shows a flow diagram of validation cohort selection. Of the 235 patients, 103 heart rhythm diagnoses (i.e., VT or SWCT) were established *with* a corroborating electrophysiological procedure (EP) or implantable intracardiac device recordings (i.e., gold standard cohort). Of the 235 patients, 132 heart rhythm diagnoses (i.e., VT or SWCT) were established *without* a corroborating EP or implantable intracardiac device recordings (i.e., non-gold standard cohort). Patient data acquisition and analysis was approved by the Human Research Protection Office of Washington University in St. Louis, Missouri.

2.4 | Heart rhythm diagnoses

Heart rhythm diagnoses (i.e., VT or SWCT) were established by the patient's supervising physician. Physicians responsible for clinical diagnoses were stratified according to a hierarchy of clinical expertise:

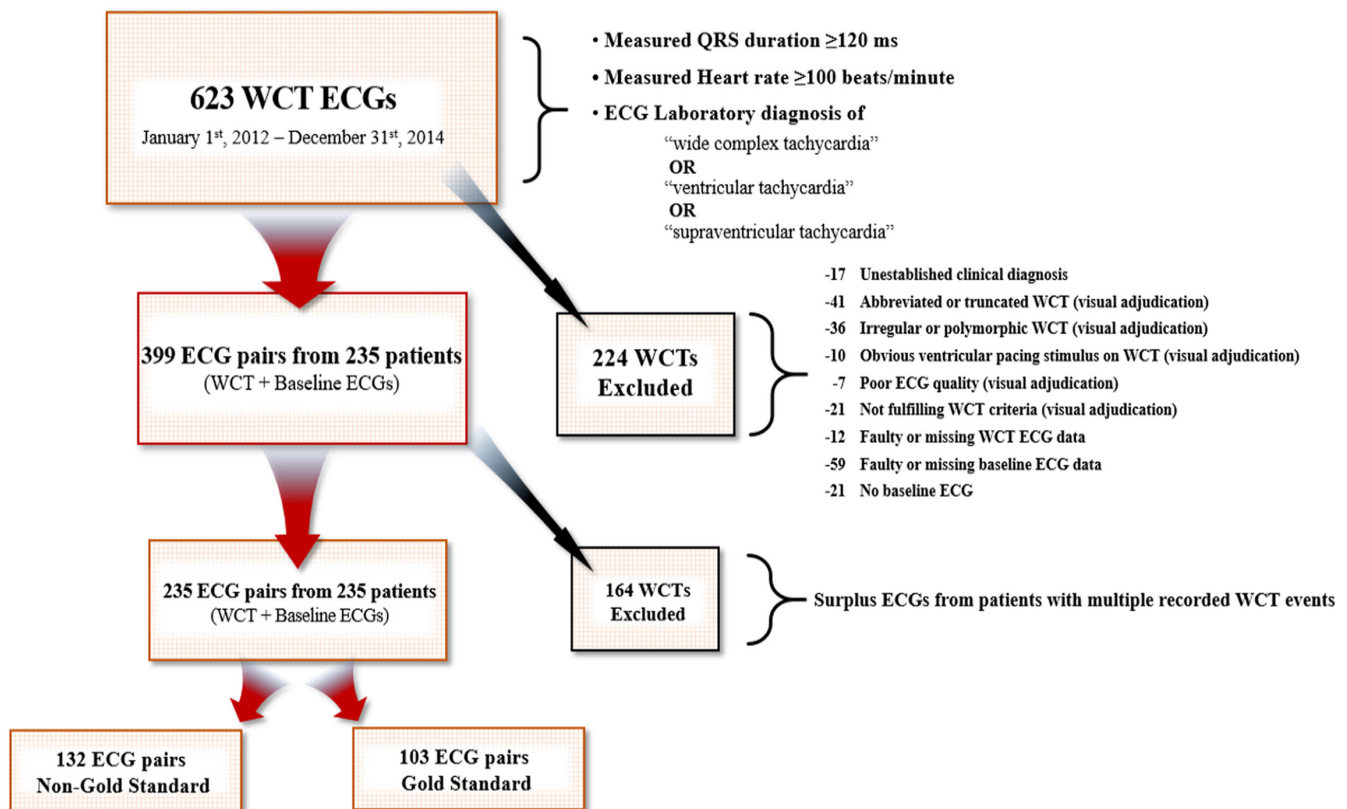


FIGURE 1 Selection of WCT ECGs. Flow diagram depicting WCT ECG cohort selection. ECG, electrocardiogram; WCT, wide complex tachycardia

(i) heart rhythm cardiologist, (ii) non-heart rhythm cardiologist, and (iii) non-cardiologist. Heart rhythm diagnoses were organized according to whether they were supported by a corroborating EP or implantable intracardiac device recordings (i.e., gold standard cohort vs. non-gold standard cohort).

2.5 | Computerized ECG measurements

Standard computerized ECG measurements for WCT and baseline ECGs, including QRS duration (ms), QRS axis ($^{\circ}$), and T-wave axis ($^{\circ}$) were automatically generated by GE Healthcare's MUSE ECG interpretation software. Computerized QRS amplitude (μV) and TVA (time-voltage area [$\mu\text{V}\cdot\text{ms}$]) measurements of waveforms above (r/R and r'/R') and below (q/QS , s/S , and s'/S') the isoelectric baseline were automatically derived from the dominant QRS complex template of each lead of the 12-lead ECG (Figure 2). Only amplitude and TVA measurements representative of QRS complex waveforms were analyzed. Measurements of the ventricular pacing stimuli or ECG artifact were excluded from our analysis.

2.6 | WCT differentiation parameters

2.6.1 | Percent monophasic time-voltage area (%)

PMonoTVA is the percentage (%) of QRS TVA contained by monophasic QRS complexes on the 12-lead ECG. This parameter is calculated as the percentage ratio of the sum of QRS TVA from ECG leads with monophasic QRS complexes (i.e., monophasic TVA) to the entire sum of QRS TVA from all ECG leads (i.e., monophasic TVA + multiphasic TVA) (Figure 3). Representative TVA measurements are attained from QRS complex waveforms (q/QS , r/R , s/S , r'/R' , and s'/S') of the dominant QRS complex template of individual leads of the 12-lead ECG.

2.6.2 | Frontal and horizontal percent amplitude changes (%)

Frontal and horizontal PACs are quantifiable measures of QRS amplitude change between paired WCT and baseline ECG recordings

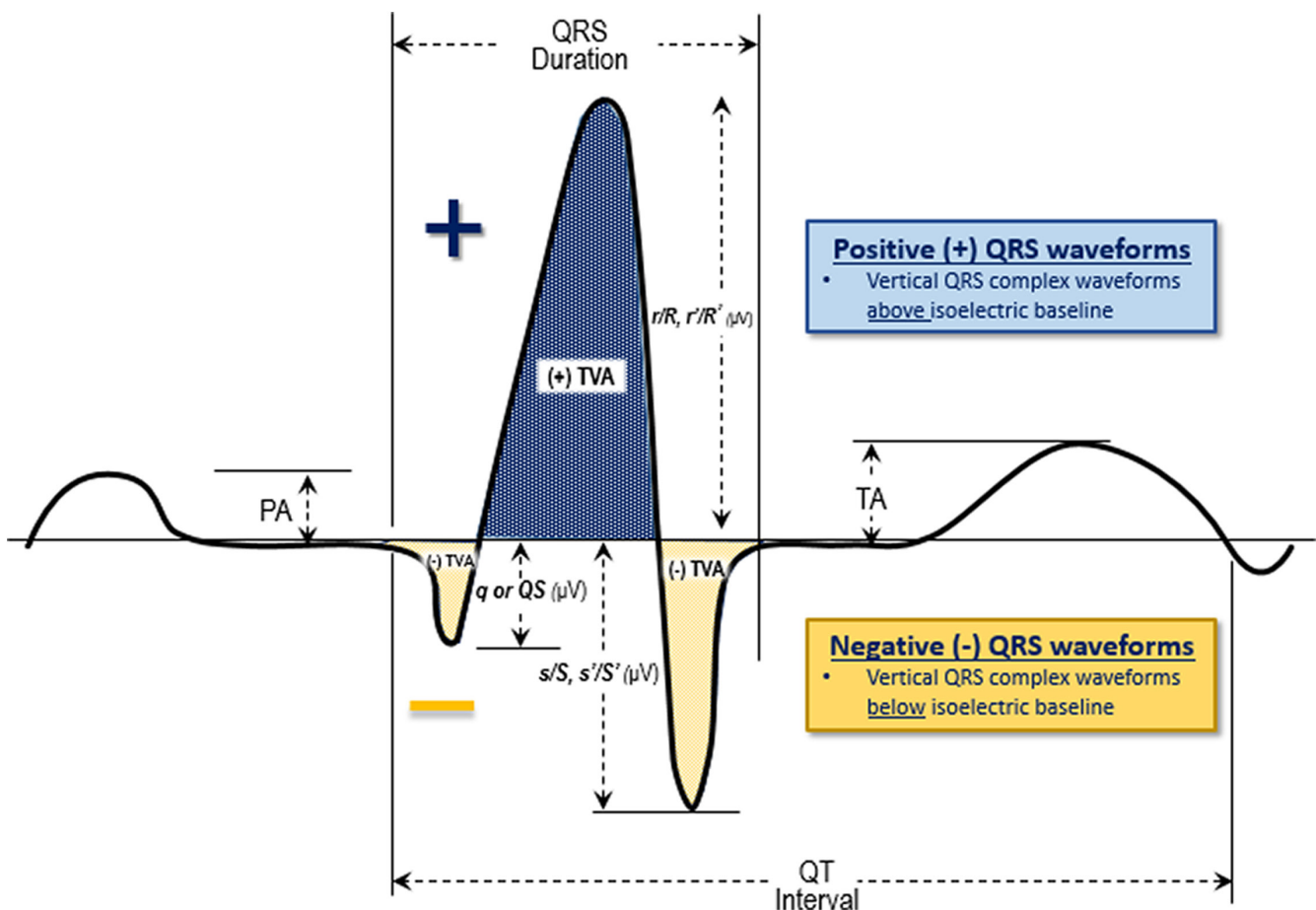


FIGURE 2 QRS complex waveform measurements. Schematic representation of a stereotypical QRS complex and its measurable components provided by computerized ECG interpretation software. QRS amplitude (μV) represents the vertical height of positive (r/R and r'/R') and negative (q/QS , s/S , and s'/S') QRS waveforms. QRS time-voltage areas (TVAs) ($\mu\text{V}\cdot\text{ms}$) represents the "area" enveloped by individual QRS complex waveforms above (r/R and r'/R') or below (q/QS , s/S , and s'/S') the isoelectric baseline. PA, p-wave amplitude; TA, T-wave amplitude; TVA, time-voltage area

Percent Monophasic time-voltage area (PMonoTVA)

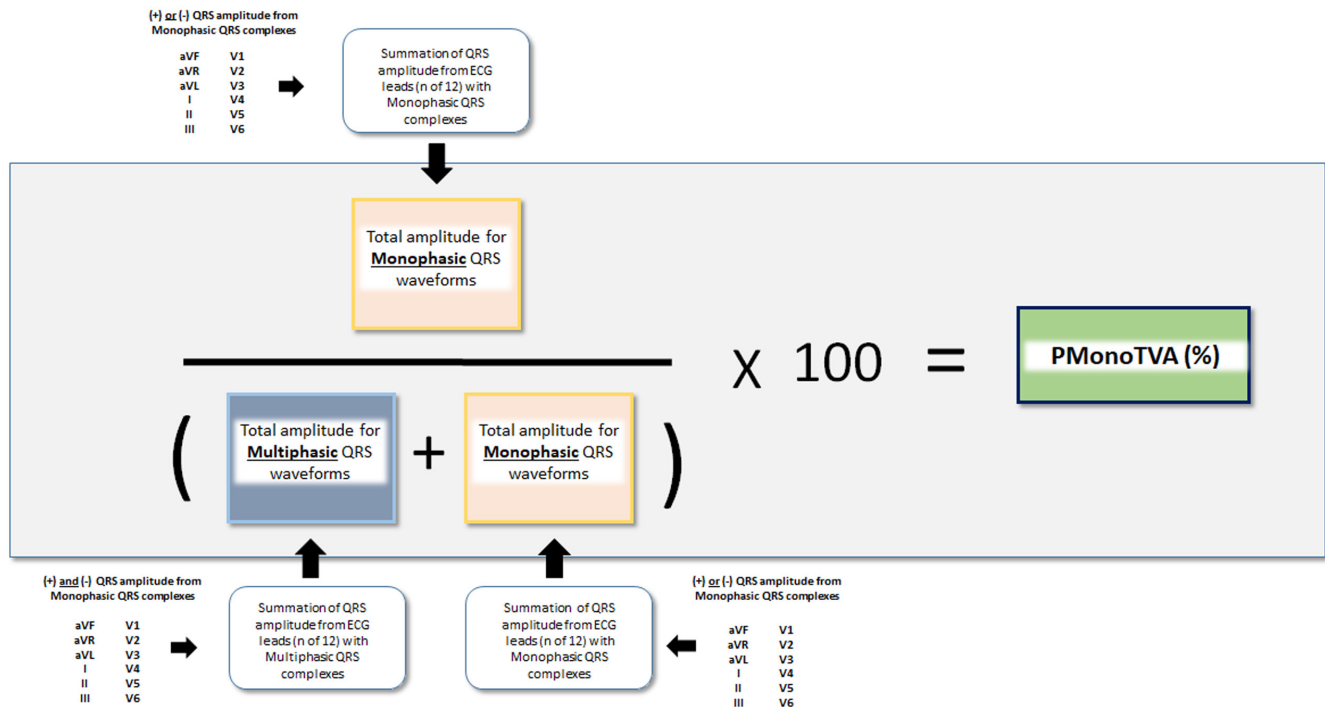


FIGURE 3 Percent monophasic time-voltage area calculation. PMonoTVA calculation is derived from measured QRS waveform TVA (time-voltage areas) ($\mu\text{V}\cdot\text{ms}$) of the dominant QRS complex template within each lead of the 12-lead ECG. ECG, electrocardiogram; PMonoTVA, percent monophasic time voltage area; TVA, time voltage area; WCT, wide complex tachycardia

(Figure S1 and S2) (May et al., 2019a, 2019b). They are derived from computerized QRS waveform (q/QS , r/R , s/S , r'/R' , and s'/S') amplitude (μV) measurements from corresponding ECG leads of the frontal (aVR, aVL, and aVF) and horizontal (V1, V4, and V6) ECG planes, respectively.

2.6.3 | Frontal and horizontal percent time-voltage area change (%)

Frontal and horizontal PTVACs are quantifiable measures of the degree of change in QRS TVA (time-voltage area) between paired WCT and baseline ECGs (Figure S3 and S4) (Kashou, DeSimone, Deshmukh, et al., 2020). They are derived from QRS complex waveform (q/QS , r/R , s/S , r'/R' , and s'/S') TVA measurements from specific ECG leads within the corresponding frontal (aVR, aVL, and aVF) or horizontal (V1, V4, and V6) ECG planes, respectively.

2.6.4 | WCT QRS duration (ms) and baseline QRS duration (ms)

QRS duration (ms) measurements for both the WCT and baseline ECGs were directly obtained from GE Healthcare's MUSE ECG interpretation software.

2.6.5 | QRS duration change (ms)

QRS duration change denotes the absolute difference in QRS duration (ms) measurements between paired WCT and baseline ECGs (May et al., 2020).

2.6.6 | QRS axis change ($^{\circ}$)

QRS axis change is the absolute difference in the frontal plane QRS axis ($^{\circ}$) between paired WCT and baseline ECGs (May et al., 2020).

2.6.7 | T-wave axis change ($^{\circ}$)

T-wave axis change represents the absolute difference in the frontal plane T-wave axis ($^{\circ}$) between paired WCT and baseline ECGs (May et al., 2020).

2.7 | Statistical analysis

In Part 1, the derivation cohort was used to generate and evaluate five different binary classification models: (i) LR (ii) artificial neural network (ANN), (iii) Random Forests (RF), (iv) support vector machine

(SVM), and (v) ensemble learning (EL). The EL model is the collective average of VT probabilities from the LR, ANN, RF, and SVM models. Other specific details relating to the structure of ML modeling techniques can be found in Table S1. Each of the five models integrated 10 parameters: PMonoTVA (%), baseline, QRS duration (ms), WCT QRS duration (ms), QRS duration change (ms), QRS axis change (°), T-wave axis change (°), frontal PAC (%), horizontal PAC (%), frontal PTVAC (%), and horizontal PTVAC (%). All methods were repeatedly (100 times) trained and validated (70/30 split), each time outputting performance measures for the validated set (i.e., accuracy, sensitivity, specificity, and AUC). In the trained data, 10-fold cross-validation was used for tuning parameter selection. After model comparison, a multivariate LR model (i.e., Paired Model), using paired WCT and baseline ECG data, was generated for its application on the validation cohort (in Part 2) due to its simplicity, ease of interpretation, and good performance. Given that only two parameters could be derived from the WCT ECG alone, a simple LR model (i.e., Solo Model) was generated to be trialed on the validation cohort (in Part 2).

In Part 2, two LR models (i.e., Solo Model and Paired Model) were applied to 103 and 132 patients with gold standard and non-gold standard diagnoses of the validation cohort, respectively. The Paired Model incorporated seven parameters (i.e., PMonoTVA [%], WCT QRS duration [ms], T-wave axis change [°], frontal PTVAC [%], horizontal PTVAC [%], frontal PAC [%], and horizontal PAC [%]) derived from data of WCT and baseline ECG pairs and the WCT ECGs alone (Figure S5). The Solo Model incorporated the only two parameters (i.e., PMonoTVA [%] and WCT QRS duration [ms]) that could be derived from WCT ECG data alone (Figure S6).

Categorical variables were compared using Chi-square tests. T-tests were used to compare normally distributed and Wilcoxon rank-sum tests were used to compare non-normally distributed continuous variables. Outlier values for modeling parameters were winsorized to diminish undue influence on model coefficients. Binary heart rhythm classification (i.e., VT or SWCT) was established using a pre-specified VT probability partition of 50% (i.e., VT ≥ 50% and SWCT < 50%). Performance metrics (i.e., accuracy, sensitivity, specificity, and AUC) for each model were assessed according to their agreement with the correct heart rhythm diagnosis (i.e., VT or SWCT). Comparison of fit between prediction models was completed using a DeLong test. The Bonferroni method was used to adjust *p*-values for multiple comparisons. A two-tailed *p* value of <0.05 was considered statistically significant. All statistical analysis was performed using R Statistical Software (R Foundation for Statistical Computing, Vienna, Austria).

3 | RESULTS

3.1 | Clinical characteristics

3.1.1 | Derivation cohort

Clinical characteristics of the derivation cohort are shown in Table 1. Among derivation cohort patients, the VT group included more

TABLE 1 Characteristics of the derivation cohort^a

Derivation cohort	SWCT (n = 242)	VT (n = 179)	<i>p</i> -value
Diagnosing provider			
Cardiologist	84 (34.7)	16 (8.9)	<.001
Heart rhythm cardiologist	92 (38.0)	155 (86.6)	
Non-cardiologist	66 (27.3)	8 (4.5)	
Patient age			
69.88 (14.85)	70 (15)	66 (14)	.006
Clinical characteristics			
Coronary artery disease	116 (47.9)	121 (67.6)	<.001
Prior myocardial infarction	63 (26.0)	102 (57.0)	<.001
Prior cardiac surgery	92 (38.0)	75 (41.9)	.481
Congenital heart disease	16 (6.6)	12 (6.7)	1.0
Anti-arrhythmic drug use	36 (14.9)	97 (54.2)	<.001
Ischemic cardiomyopathy	38 (15.7)	89 (49.7)	<.001
Non-ischemic cardiomyopathy	53 (21.9)	54 (30.2)	.07
ICD	17 (7.0)	112 (62.6)	<.001
Pacemaker	18 (7.4)	4 (2.2)	.032
Left ventricular ejection fraction (%)			
LVEF (>50)	140 (57.9)	48 (26.8)	<.001
LVEF (49–31)	48 (19.8)	60 (33.5)	
LVEF (≤30)	42 (17.4)	70 (39.1)	
LVEF unknown	12 (5.0)	1 (0.6)	
Gold standard diagnosis			
Yes	63 (26.0)	129 (72.1)	<.001

Abbreviations: ECG, electrocardiogram; ICD, implantable cardioverter-defibrillator; SWCT, supraventricular tachycardia; VT, ventricular tachycardia.

^aNumbers in parentheses are percent (%) of *n* or standard deviation. Patients having a gold standard diagnosis were those with a corroborating EP or implantable intracardiac device recordings.

patients with coronary artery disease, prior myocardial infarction, ongoing antiarrhythmic drug use, ischemic cardiomyopathy, and an implantable cardioverter-defibrillator (ICD). The SWCT group included more patients with an implanted pacemaker. The VT group comprised more patients with a severely depressed (≤30%) left ventricular ejection fraction (LVEF), whereas the SWCT group included more patients with a preserved (≥50%) LVEF. A majority of patients with VT diagnoses had a corroborating EP or intracardiac device recording. Conversely, a minority of SWCT patients had a corroborating EP or intracardiac device recording.

3.1.2 | Validation cohort

Clinical characteristics of the validation cohort are shown in Table 2. Among validation cohort patients, the VT group included more patients with ongoing antiarrhythmic drug use, ischemic

TABLE 2 Characteristics of the validation cohort^a

Validation cohort	SWCT (n = 158)	VT (n = 77)	p-value
Diagnosing provider			
Cardiologist	77 (48.7)	29 (37.7)	.001
Heart rhythm cardiologist	36 (22.8)	35 (45.5)	
Non-cardiologist	45 (28.5)	13 (16.9)	
Patient age			
	65 (15)	64 (14)	.705
Clinical characteristics			
Coronary artery disease	83 (52.5)	44 (57.1)	.599
Prior myocardial infarction	71 (44.9)	43 (55.8)	.152
Prior cardiac surgery	33 (20.9)	26 (33.8)	.048
Congenital heart disease	8 (5.1)	2 (2.6)	.593
Anti-arrhythmic drug use	45 (28.7)	46 (59.7)	<.001
Ischemic cardiomyopathy	55 (34.8)	41 (53.2)	.011
Non-ischemic cardiomyopathy	54 (34.2)	29 (37.7)	.704
ICD	37 (23.4)	47 (61.0)	<.001
Pacemaker	7 (4.4)	0 (0.0)	.143
Left ventricular ejection fraction (%)			
LVEF (≥50)	68 (43.0)	10 (13.0)	<.001
LVEF (49–31)	38 (24.1)	18 (23.4)	
LVEF (≤30)	47 (29.7)	48 (62.3)	
LVEF unknown	5 (3.2)	1 (1.3)	
Gold standard diagnosis			
Yes	55 (34.2)	48 (64.9)	<.001

Abbreviations: ECG, electrocardiogram; ICD, implantable cardioverter-defibrillator; SWCT, supraventricular tachycardia; VT, ventricular tachycardia.

^aNumbers in parentheses are percent (%) of *n* or standard deviation. Patients having a gold standard diagnosis were those with a corroborating EP or implantable intracardiac device recordings.

cardiomyopathy, and an ICD. Similar to the derivation cohort, the VT group comprised more patients with a severely depressed (≤30%) LVEF, while the SWCT group included more patients with a preserved (≥50%) LVEF. Similar to the derivation cohort, most VT patients, and a minority of SWCT patients, had a corroborating EP or intracardiac device recording.

3.2 | WCT differentiation parameters

Table 3 summarizes WCT differentiation parameter values across VT and SWCT groups for the validation cohort. The VT group expressed greater PMonoTVA, WCT QRS duration, QRS duration change, QRS axis change, T-wave axis change, frontal PAC, horizontal PAC, frontal PTVAC, and horizontal PTVAC. The median and proportional distribution of PMonoTVA among VT and SWCT groups is shown in Figure 4.

3.3 | Part 1: Diagnostic performance of WCT differentiation model subtypes

Diagnostic performance metrics of the five binary classification models, when applied to the derivation cohort, is summarized in Table 4. Overall, each model subtype demonstrated similar diagnostic performance.

3.4 | Part 2: Solo model versus paired model

Diagnostic performance metrics of the Solo Model and Paired Model is summarized in Table 5 and Figure 5. The Paired Model demonstrated superior overall accuracy, sensitivity, specificity, and AUC compared to Solo Model across the gold standard and non-gold standard study cohorts ($p < .0001$).

4 | DISCUSSION

4.1 | WCT differentiation model performance

In this work, we developed and evaluated novel automated WCT differentiation models capable of accurately distinguishing VT and SWCT. In Part 1, we demonstrated comparable diagnostic performance among various ML techniques (LR modeling included) using a broad collection of WCT differentiation parameters. In Part 2, we validated two novel LR models, each with different application constraints (i.e., WCT ECG data alone [Solo Model] vs. WCT and baseline ECG data [Paired Model]), on separate data using patients from a different institution. The Paired Model (using paired WCT and baseline ECG data) demonstrated superior overall accuracy, sensitivity, specificity, and AUC compared with Solo WCT Model (using WCT ECG data alone).

4.2 | Novel WCT differentiation parameter: PMonoTVA

Central to this analysis was the integration of a novel WCT differentiation parameter (i.e., PMonoTVA) representing the proportion of QRS TVA contained by monophasic QRS complexes found on the WCT ECG. We observed greater PMonoTVA values among patients with VT as compared patients with SWCT. The conceptual basis for this parameter helping differentiate WCTs relates to the manner in which ventricular depolarization most commonly occurs for VT and SWCT.

4.2.1 | Ventricular depolarization by ventricular tachycardia

For most VTs, ventricular depolarization wavefronts spread from their site-of-origin (SOO) using cardiomyocyte-to-cardiomyocyte

	WCT (n = 235)	SWCT (n = 158)	VT (n = 77)	p-value
PMonoTVA (%)	23.6 (5.5, 58.4)	11.7 (0.0, 36.6)	55.6 (35.4, 74.2)	<.001
Baseline QRS duration (ms)	132.0 (112.0, 154.0)	134.0 (114.0, 152.0)	128.0 (110.0, 164.0)	.884
WCT QRS duration (ms)	146.0 (132.0, 162.0)	140.0 (128.0, 152.0)	162.0 (144.0, 186.0)	<.001
QRS duration change (ms)	16.0 (6.0, 44.0)	12.0 (4.50, 27.5)	44.0 (16.0, 62.0)	<.001
QRS axis change (°)	23.0 (8.0, 73.0)	12.5 (4.0, 34.5)	89.0 (45.0, 127.0)	<.001
T axis change (°)	42.0 (14.0, 103.0)	23.0 (9.0, 51.0)	104.0 (71.0, 142.0)	<.001
Frontal PAC (%)	52.4 (24.3, 96.9)	29.7 (18.2, 55.4)	110.3 (81.0, 149.1)	<.001
Horizontal PAC (%)	57.7 (36.8, 97.8)	41.6 (26.4, 67.4)	111.8 (74.3, 140.2)	<.001
Frontal PTVAC (%)	59.9 (29.0, 145.0)	35.5 (23.0, 66.6)	163.8 (127.8, 285.3)	<.001
Horizontal PTVAC (%)	72.5 (39.1, 153.8)	54.3 (30.9, 82.2)	168.5 (115.0, 238.6)	<.001

TABLE 3 WCT differentiation parameters^a

Abbreviations: PAC, percent amplitude change; PMonoTVA, percent monophasic time voltage area; PTVAC, percent time-voltage area change; SWCT, supraventricular tachycardia; VT, ventricular tachycardia; WCT, wide complex tachycardia.

^aDisplayed numbers represent mean values. Numbers in parentheses are interquartile ranges.

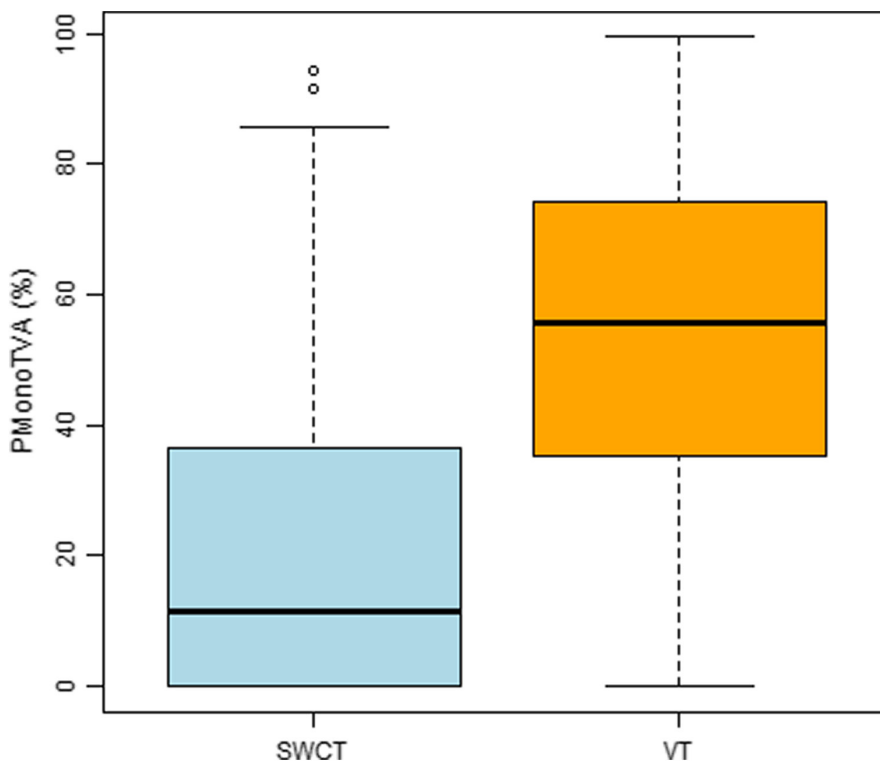


FIGURE 4 PMonoTVA (%). Box-plot demonstrating the median and proportional distribution of PMonoTVA (%). PMonoTVA, percent monophasic time voltage area; SWCT, supraventricular wide complex tachycardia; VT, ventricular tachycardia

conduction, with little-to-no assistance from the specialized conduction tissue (Figure 6). As a result, the VT ventricular depolarization wavefronts tend to spread homogeneously without rapid engagement and subdivision along an arborized His-Purkinje network.

Without engagement of specialized conduction tissue, VT will seldom create diametrically opposed and temporally separated QRS complex waveforms. Rather, patients with VT will often demonstrate monophasic QRS complexes (i.e., monophasic “QS complexes”

TABLE 4 Diagnostic performance of WCT differentiation model subtypes^a

	Accuracy (%)	Sensitivity (%)	Specificity (%)	AUC
Logistic regression	90 (88–90)	87 (85–89)	92 (90–93)	0.96 (0.96–0.97)
Artificial neural network	90 (89–91)	89 (85–91)	92 (89–93)	0.96 (0.96–0.97)
Random forest	90 (85–94)	88 (74–96)	91 (82–97)	0.96 (0.92–0.99)
Support vector machine	90 (85–95)	89 (80–98)	91 (85–97)	0.96 (0.93–0.99)
Ensemble learner	90 (85–95)	89 (80–96)	91 (83–97)	0.97 (0.93–0.99)

Abbreviation: AUC, area under the curve.

^aSummary of the diagnostic performance of various WCT differentiation model subtypes. Displayed numbers represent mean values. Numbers in parentheses are interquartile ranges.

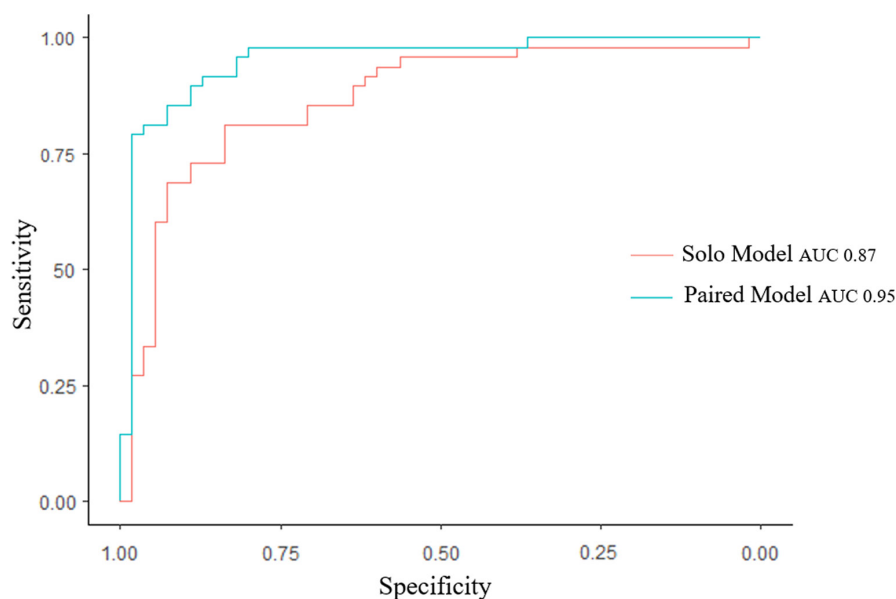
TABLE 5 Solo model and paired model diagnostic performance^a

	Cohort	Accuracy (%)	Sensitivity (%)	Specificity (%)	AUC
Solo model	Gold standard	82	79	84	0.87
	Non-gold standard	80	54	87	0.84
Paired model	Gold standard	88	83	93	0.95
	Non-gold standard	89	88	90	0.95

Abbreviation: AUC, area under the receiver operator curve.

^aSummary of solo model and paired model diagnostic performance across the gold standard and non-gold standard cohort.

FIGURE 5 Solo model versus paired model. ROC curve with the solo model versus paired model as applied to the gold-standard group of the validation cohort. AUC, area under the receiver operating characteristic curve



for ventricular depolarization wavefronts propagating away from any of the 12 ECG leads or monophasic “R complexes” propagating towards any of the any of the 12 ECG leads) (Figure S7), especially if the SOO is remote from specialized conduction tissue or subjacent to ventricular epicardium.

4.2.2 | Ventricular depolarization by supraventricular wide complex tachycardia

In contrast to VT, most SWCT subtypes rely heavily upon the heart’s specialized conduction tissue—not only as the primary link

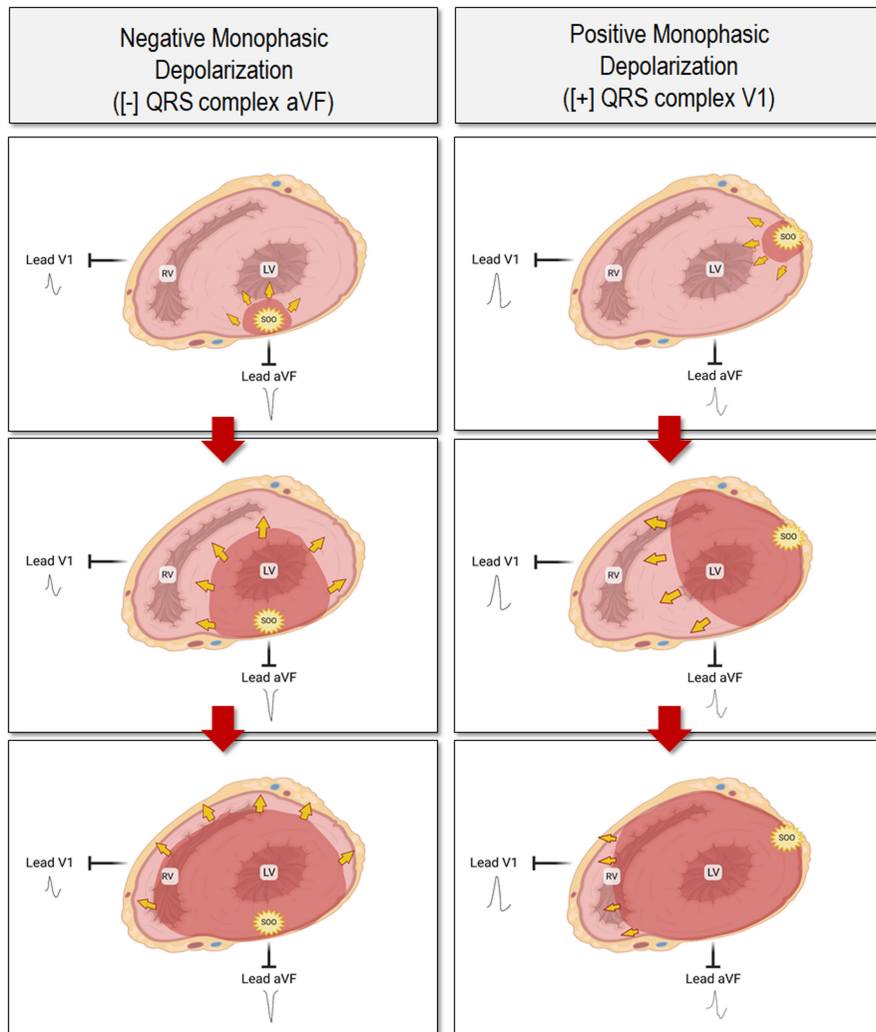


FIGURE 6 Ventricular tachycardia: Ventricular depolarization producing monophasic QRS complexes. Illustration of the development of monophasic QRS complexes due to VT. Left panels demonstrate the development of a negative monophasic QRS complex in lead aVF. Right panels demonstrate the development of a positive monophasic QRS complex in lead V1. Each panel series (A to B to C) demonstrates the progression ventricular depolarization wavefronts that spread uniformly from the site-of-origin. Embedded yellow arrows depict the directionality of ventricular depolarization. Red shading represents depolarized myocardium. LV, left ventricle; RV, right ventricle; SOO, site-of-origin. Created with BioRender.com

that couples supraventricular impulses to ventricular depolarization but also as the indispensable conduit by which biventricular depolarization is accomplished. Among SWCTs arising from aberrant conduction (e.g., left bundle branch block [LBBB] or right bundle branch block [RBBB]), the rapid initial stages of ventricular depolarization, affected by propagation through specialized conduction tissue, is subsequently followed by a slower ventricular depolarization wavefront, which primarily relies upon slower cardiomyocyte-to-cardiomyocyte conduction (Figure 7). As a result, the different and temporally distinct components of ventricular depolarization (i.e., initial vs. late) tend manifest multiphasic QRS complexes having diametrically opposed and temporally separated QRS complex waveform components (i.e., positive [+] QRS waveforms [r/R, r'/R'] vs. negative [-] QRS waveforms [q/Q, s/S, s'/S']) (Figure S8).

4.3 | Established WCT differentiation parameters

4.3.1 | WCT QRS duration and absolute change in QRS duration

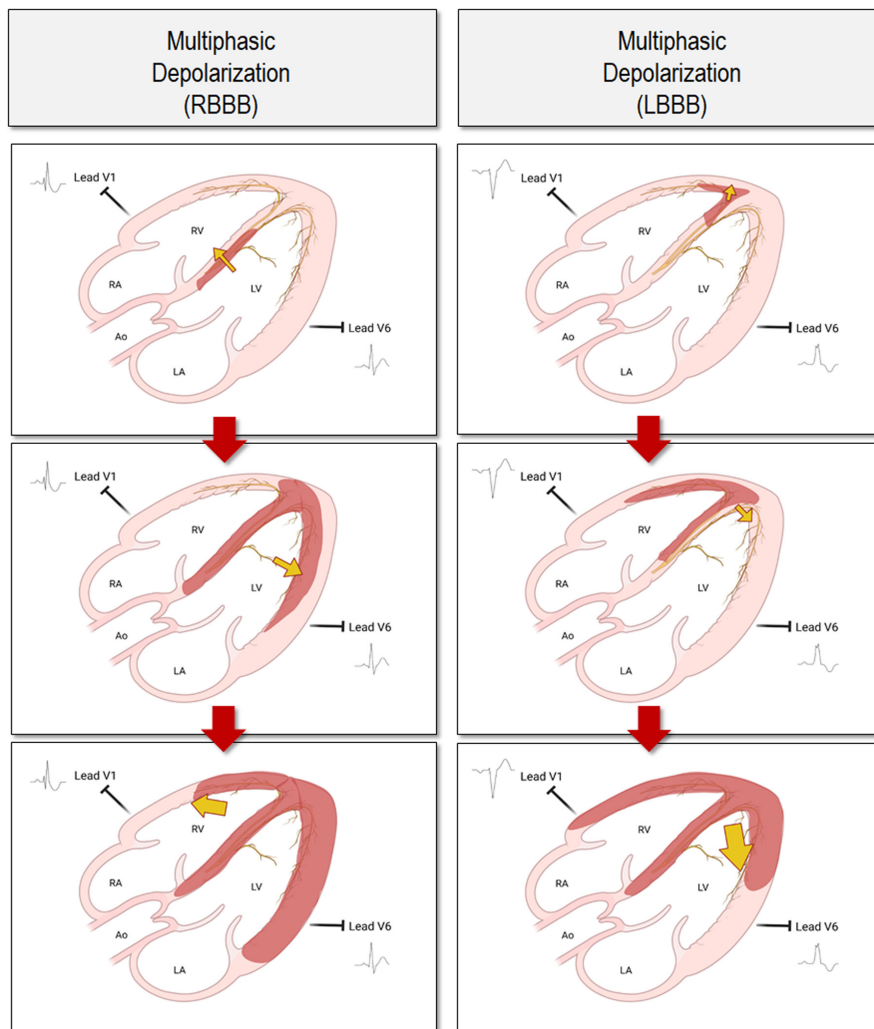
We observed that patients presenting with VT demonstrate greater WCT QRS duration and absolute change in QRS duration

than patients with SWCT. These findings are in agreement with a prior study (May et al., 2020) that demonstrated that parameters relating to QRS duration (i.e., WCT QRS duration, baseline QRS duration, and absolute change in QRS duration) are quite useful in differentiating WCTs. Our findings reinforce the concept that WCTs having greater WCT QRS duration, baseline QRS duration, and absolute change in QRS duration are more likely VT, while WCTs demonstrating lesser values are more likely SWCT.

4.3.2 | QRS axis change and T-wave axis change

We observed WCTs exhibiting larger QRS axis and T axis changes compared to the baseline rhythm were more likely VT, while WCTs demonstrating smaller QRS axis and T axis changes were more likely SWCT. These findings are in agreement with a prior study (May et al., 2020) and support the concept that changes in the direction of the mean electrical vector of ventricular depolarization (i.e., QRS axis change) and/or repolarization (i.e., T axis change) are valuable in differentiating the underlying WCT rhythm (i.e., VT or SWCT)—that is, large changes predict VT and smaller changes predict SWCT (Evenson et al., 2021).

FIGURE 7 Supraventricular wide complex tachycardia: Ventricular depolarization producing multiphasic QRS complexes. Illustration of the development of multiphasic QRS complexes due to SWCT with aberrancy. Left panels demonstrate the creation of multiphasic QRS complex in leads V1 and V6 due to RBBB. Right panels demonstrate the creation of multiphasic QRS complex in leads V1 and V6 due to LBBB. Each panel series (A to B to C) demonstrates the progression ventricular depolarization wavefronts that stereotypically occur for RBBB (left panels) and LBBB (right panels). Embedded yellow arrows depict the directionality and intensity of mean electrical vector during ventricular depolarization. Red shading represents depolarized myocardium. Ao, aorta; LA, left atrium; LBBB, left bundle branch block; LV, left ventricle; RA, right atrium; RBBB, right bundle branch block; RV, right ventricle. Created with BioRender.com



4.3.3 | Percent amplitude change and percent time-voltage area change

Frontal and horizontal PAC and PTVAC are novel calculations that broadly quantify the extent of QRS amplitude and TVA changes between WCT and baseline ECGs, respectively. In this work, we observed that WCTs exhibiting larger frontal and horizontal PAC and PTVAC were more likely VT while WCTs demonstrating smaller frontal and horizontal PAC and PTVAC were more likely SWCT. These findings are in agreement with prior investigations (Kashou et al., 2021; Kashou, DeSimone, Deshmukh, et al., 2020; May et al., 2019a) that demonstrated paired WCT and baseline ECGs with greater frontal and/or horizontal PAC and PTVAC values were more commonly associated with VT.

The aforementioned observations may be explained by the differences by which VT and SWCT ordinarily depolarize the ventricular myocardium (Evenson et al., 2021). In general, VT categorically demonstrates greater number of possibilities in the manner to which ventricular depolarization may occur compared to its relatively constrained SWCT counterpart. Thus, the broad expanse of VT manifestations can yield a vastly greater number of distinct QRS complexes

than what can develop from SWCT, which in turn can translate into larger QRS amplitude and TVA changes for VT compared to SWCT.

4.4 | Prospective clinical applications

Ideally, accurate and reliable separation of VT and SWCT would occur immediately upon 12-lead ECG acquisition. Unfortunately, automated ECG interpretation software programs have not yet achieved sufficient diagnostic accuracy for interpretation of many complex heart rhythms (Schlapfer & Wellens, 2017), including WCTs. Current computerized ECG interpretation software does not reliably differentiate VT and SWCT; instead, in most circumstances, recorded WCTs are simply given the general label “wide complex tachycardia,” thereby providing little diagnostic assistance to clinicians. Thus, clinicians must rely on traditional manual ECG interpretation methods and techniques, which universally have inherent limitations relating to their application (Kashou, Noseworthy, DeSimone, et al., 2020).

Several studies (Kashou et al., 2021; Kashou, DeSimone, Deshmukh, et al., 2020; May et al., 2019a, 2020) have introduced novel automated approaches to differentiate WCTs using computerized

ECG interpretation software, each offering a compelling option that avoids the practical and diagnostic limitations inextricably associated with manual ECG interpretation methods. Recently, a separate analysis has confirmed that one automated WCT differentiation model (i.e., VT Prediction Model) improved users' diagnostic performance (Kashou et al., 2022). By design, automated methods transform computerized ECG data, which is routinely processed by ECG interpretation software programs, into novel parameters (e.g., frontal and horizontal PTVAC) that can be integrated into binary classification modeling techniques (i.e., LR). The central advantage of these novel WCT differentiation methods is that they can provide clinicians an immediate and unambiguous estimation of VT likelihood (i.e., 0.00% to 99.99% VT probability)—independent of clinicians' ECG interpretation expertise or competency. Therefore, clinicians could integrate the VT probability estimate along with the influence of traditional WCT differentiation methods (e.g., Brugada algorithm (Brugada et al., 1991)) or other relevant clinical information (e.g., history of VT). Lastly, it is conceivable that the novel parameters described in this work may be used to create novel algorithms that also take into account clinical information, similar to the approach recently described by Moccetti and colleagues (Moccetti et al., 2022). By these means, commercially available ECG interpretation software platforms could more adeptly assist clinicians in distinguishing VT and SWCT accurately and, hopefully, transform a once historically challenging clinical task into an outmoded diagnostic problem.

Until now, a universal limitation of automated WCT differentiation methods is that they require computerized data provided by *both* the WCT ECG and its corresponding baseline ECG. In this work, we developed a novel means to distinguish VT and SWCT accurately using ECG data solely provided by WCT. The so-called Solo WCT Model makes use of two highly predictive parameters derived solely from the WCT ECG: (i) a standard and universally reported ECG measurement (i.e., WCT QRS duration) and (ii) a novel computationally derived parameter (i.e., PMonoTVA). As such, the Solo WCT Model can deliver accurate VT probability estimates any time a WCT is recorded by a 12-lead ECG—even in the absence of a baseline ECG. In addition, Solo WCT Model application can be coordinated with other high-performing models that require computerized data from paired WCT and baseline ECGs (Figures S9 and S10). For instance, once a previously absent baseline ECG is recorded after the WCT event, the Paired Model can proceed with its application to provide a more robust VT probability estimate. However, if a patient already possesses a digitally archived baseline ECG that is available for automated WCT differentiation algorithm application, VT or SWCT classification (or VT probability estimation) may be executed by models that leverage paired WCT and baseline ECG comparisons, and thereby supersede the classification or VT probability predictions attained by the Solo Model, which only analyzes computerized ECG data provided by the WCT itself.

4.5 | Study limitations

This study is best evaluated in the context of its limitations. First, our study examined any patient with a clinically encountered WCT that

was formally diagnosed by the patient's overseeing physician. As a result, our study evaluated WCTs *with* and *without* a corroborating EP or implanted intra-cardiac device recording. Although we found Solo WCT Model and Paired Model performed well on gold standard and non-gold standard cohorts, we acknowledge that a significant proportion of this analysis includes VT or SWCT diagnoses not established by the traditional “gold standard.” Second, as our analysis examined 12-lead ECGs acquired within clinical settings, we cannot make more exhaustive conclusions regarding automated model performance among various SWCT (e.g., SWCT due to bystander conduction over accessory pathways) and VT (e.g., fascicular VT) subtypes. Characterization of various VT and SWCT subtypes would require review of WCT heart rhythms recorded during an electrophysiology procedure. Nevertheless, by deliberately evaluating “all comers” who presented with a WCT captured by the 12-lead ECG in genuine clinical circumstances, and not just a minority of WCT patients who have their VT or SWCT diagnoses confirmed by the conventional “gold standard,” the performance achieved by the novel automated models are more generalizable for broader clinical use. Lastly, the diagnostic performance of automated models were not directly compared with traditional manual WCT differentiation approaches. Additional research is necessary to determine whether automated models exhibit diagnostic superiority over traditional manual interpretation methods.

5 | CONCLUSION

Accurate automatic WCT differentiation may be accomplished through the use of novel parameters derived from computerized data of the (i) WCT ECG alone and (ii) paired WCT and baseline ECGs. Once automated WCT differentiation models are integrated into commercially available computerized ECG interpretation software, they may help clinicians distinguish VT and SWCT accurately.

AUTHOR CONTRIBUTIONS

Anthony H. Kashou: Investigation, methodology, writing – original draft, writing – review and editing. **Sarah LoCoco:** Writing – review and editing, data curation. **Preet A. Shaikh:** Writing – review and editing. **Bhavesh B. Katbamna:** Writing – review and editing. **Ojasav Sehrawat:** Writing – review and editing. **Daniel H. Cooper:** Writing – review and editing. **Sandeep S. Sodhi:** Writing – review and editing. **Phillip S. Cuculich:** Writing – review and editing. **Mary J. Gleva:** Writing – review and editing. **Elena Deych:** Formal analysis, methodology, writing – review and editing. **Ruiwen Zhou:** Formal analysis, methodology, writing – review and editing. **Lei Liu:** Formal analysis, methodology, writing – review and editing. **Abhishek J. Deshmukh:** Writing – review and editing. **Samuel J. Asirvatham:** Writing – review and editing. **Peter A. Noseworthy:** Writing – review and editing. **Christopher V. DeSimone:** Writing – review and editing. **Adam M. May:** Conceptualization, data curation, funding acquisition, investigation, methodology, writing – original draft, project administration, writing – review and editing.

CONFLICT OF INTEREST

Authors, Adam May, Anthony Kashou, Chris DeSimone, and Abhishek Deshmukh are obliged to disclose that they are "would-be" beneficiaries of intellectual property that relates to this manuscript's content. The technology(s) discussed in this manuscript was disclosed Mayo Clinic Ventures or Office of Technology Management at Washington University in St. Louis.

DATA AVAILABILITY STATEMENT

The data that support the findings of this study are available from the corresponding author upon reasonable request.

ETHICS STATEMENT

This paper reflects the authors' own research and analysis. This research was conducted in a truthful and transparent manner.

ORCID

Adam M. May  <https://orcid.org/0000-0002-4120-5075>

REFERENCES

- Akhtar, M., Shenasa, M., Jazayeri, M., Caceres, J., & Tchou, P. J. (1988). Wide QRS complex tachycardia: Reappraisal of a common clinical problem. *Annals of Internal Medicine*, *109*, 905–912.
- Baxi, R. P., Hart, K. W., Vereckei, A., Miller, J., Chung, S., Chang, W., Gottesman, B., Hunt, M., Culyer, G., Trimarco, T., Willoughby, C., Suarez, G., Lindsell, C. J., & Collins, S. P. (2012). Vereckei criteria used as a diagnostic tool by emergency medicine residents to distinguish between ventricular tachycardia and supra-ventricular tachycardia with aberrancy. *Journal of Cardiology*, *59*, 307–312.
- Brugada, P., Brugada, J., Mont, L., Smeets, J., & Andries, E. W. (1991). A new approach to the differential diagnosis of a regular tachycardia with a wide QRS complex. *Circulation*, *83*, 1649–1659.
- Chen, Q., Xu, J., Gianni, C., Trivedi, C., Della Rocca, D. G., Bassiouny, M., Canpolat, U., Tapia, A. C., Burkhardt, J. D., Sanchez, J. E., Hranitzky, P., Gallinghouse, G. J., al-Ahmad, A., Horton, R., di Biase, L., Mohanty, S., & Natale, A. (2019). Simple electrocardiographic criteria for the rapid identification of wide QRS complex tachycardia: The new limb lead algorithm. *Heart Rhythm*, *17*, 431–438.
- Evenson, C. M., Kashou, A. H., LoCoco, S., DeSimone, C. V., Deshmukh, A. J., Cuculich, P. S., Noseworthy, P. A., & May, A. M. (2021). Conceptual and literature basis for wide complex tachycardia and baseline ECG comparison. *Journal of Electrocardiology*, *65*, 50–54.
- Griffith, M. J., Garratt, C. J., Mounsey, P., & Camm, A. J. (1994). Ventricular tachycardia as default diagnosis in broad complex tachycardia. *Lancet*, *343*, 386–388.
- Isenhour, J. L., Craig, S., Gibbs, M., Littmann, L., Rose, G., & Risch, R. (2000). Wide-complex tachycardia: Continued evaluation of diagnostic criteria. *Academic Emergency Medicine*, *7*, 769–773.
- Jastrzebski, M., Kukla, P., & Czarnecka, D. (2017). Ventricular tachycardia score—A novel method for wide QRS complex tachycardia differentiation—Explained. *Journal of Electrocardiology*, *50*, 704–709.
- Kashou, A. H., DeSimone, C. V., Deshmukh, A. J., McGill, T. D., Hodge, D. O., Carter, R., Cooper, D. H., Cuculich, P. S., Noheria, A., Asirvatham, S. J., & Noseworthy, P. A. (2020). The WCT formula II: An effective means to automatically differentiate wide complex tachycardias. *Journal of Electrocardiology*, *61*, 121–129.
- Kashou, A. H., DeSimone, C. V., Hodge, D. O., Carter, R., Lin, G., Asirvatham, S. J., Noseworthy, P. A., Deshmukh, A. J., & May, A. M. (2020). The ventricular tachycardia prediction model: Derivation and validation data. *Data in Brief*, *30*, 105515.
- Kashou, A. H., LoCoco, S., McGill, T. D., Evenson, C. M., Deshmukh, A. J., Hodge, D. O., Cooper, D. H., Sodhi, S. S., Cuculich, P. S., Asirvatham, S. J., & Noseworthy, P. A. (2021). Automatic wide complex tachycardia differentiation using mathematically synthesized vectorcardiogram signals. *Annals of Noninvasive Electrocardiology*, *27*, e12890.
- Kashou, A. H., Noseworthy, P. A., DeSimone, C. V., Deshmukh, A. J., Asirvatham, S. J., & May, A. M. (2020). Wide complex tachycardia differentiation: A reappraisal of the state-of-the-art. *Journal of the American Heart Association*, *9*, e016598.
- Kashou, A. H., Noseworthy, P. A., Jentzer, J. C., Rafie, N., Roy, A. R., Abraham, H. M., Sang, P. D., Kronzer, E. K., Inglis, S. S., Rezkalla, J. A., Julakanti, R. R., Saric, P., Asirvatham, S. J., Deshmukh, A. J., DeSimone, C. V., & May, A. M. (2022). Wide complex tachycardia discrimination tool improves physicians' diagnostic accuracy. *Journal of Electrocardiology*, *74*, 32–39.
- Kindwall, K. E., Brown, J., & Josephson, M. E. (1988). Electrocardiographic criteria for ventricular tachycardia in wide complex left bundle branch block morphology tachycardias. *The American Journal of Cardiology*, *61*, 1279–1283.
- Lau, E. W., Pathamanathan, R. K., Ng, G. A., Cooper, J., Skehan, J. D., & Griffith, M. J. (2000). The Bayesian approach improves the electrocardiographic diagnosis of broad complex tachycardia. *Pacing and Clinical Electrophysiology*, *23*, 1519–1526.
- Marriott, H. J. (1970). Differential diagnosis of supraventricular and ventricular tachycardia. *Geriatrics*, *25*, 91–101.
- May, A. M., Brenes-Salazar, J. A., DeSimone, C. V., Vaidya, V. R., Ternus, B. W., Hodge, D. O., Lin, G., Mulpuru, S. K., Deshmukh, A. J., Noseworthy, P. A., & Brady, P. A. (2018). Electrocardiogram algorithms used to differentiate wide complex tachycardias demonstrate diagnostic limitations when applied by non-cardiologists. *Journal of Electrocardiology*, *51*, 1103–1109.
- May, A. M., DeSimone, C. V., Kashou, A. H., Hodge, D. O., Lin, G., Kapa, S., Asirvatham, S. J., Deshmukh, A. J., Noseworthy, P. A., & Brady, P. A. (2019a). The WCT formula: A novel algorithm designed to automatically differentiate wide-complex tachycardias. *Journal of Electrocardiology*, *54*, 61–68.
- May, A. M., DeSimone, C. V., Kashou, A. H., Hodge, D. O., Lin, G., Kapa, S., Asirvatham, S. J., Deshmukh, A. J., Noseworthy, P. A., & Brady, P. A. (2019b). The wide complex tachycardia formula: Derivation and validation data. *Data in Brief*, *24*, 103924.
- May, A. M., DeSimone, C. V., Kashou, A. H., Sridhar, H., Hodge, D. O., Carter, R., Lin, G., Asirvatham, S. J., Noseworthy, P. A., & Deshmukh, A. J. (2020). The VT prediction model: A simplified means to differentiate wide complex tachycardias. *Journal of Cardiovascular Electrophysiology*, *31*, 185–195.
- Mocchetti, F., Yadava, M., Latifi, Y., Strebel, I., Pavlovic, N., Knecht, S., Asatryan, B., Schaer, B., Kühne, M., Henrikson, C. A., Stephan, F. P., Osswald, S., Sticherling, C., & Reichlin, T. (2022). Simplified integrated clinical and electrocardiographic algorithm for differentiation of wide QRS complex tachycardia: The Basel algorithm. *JACC: Clinical Electrophysiology*, *8*, 831–839.
- Pachon, M., Arias, M. A., Salvador-Montanes, O., Calvo, D., Peñafiel, P., Puchol, A., Martín-Sierra, C., Akerström, F., Pachón, N., Rodríguez-Padial, L., & Almendral, J. (2019). A scoring algorithm for the accurate differential diagnosis of regular wide QRS complex tachycardia. *Pacing and Clinical Electrophysiology*, *42*, 625–633.
- Pava, L. F., Perafan, P., Badiel, M., Arango, J. J., Mont, L., Morillo, C. A., & Brugada, J. (2010). R-wave peak time at DII: A new criterion for differentiating between wide complex QRS tachycardias. *Heart Rhythm*, *7*, 922–926.

- Sandler, I. A., & Marriott, H. J. (1965). The differential morphology of anomalous ventricular complexes of RBBB-type in Lead V1: Ventricular ectopy versus aberration. *Circulation*, *31*, 551–556.
- Schlapfer, J., & Wellens, H. J. (2017). Computer-interpreted electrocardiograms: Benefits and limitations. *Journal of the American College of Cardiology*, *70*, 1183–1192.
- Vereckei, A., Duray, G., Szenasi, G., Altemose, G. T., & Miller, J. M. (2008). New algorithm using only lead aVR for differential diagnosis of wide QRS complex tachycardia. *Heart Rhythm*, *5*, 89–98.
- Wellens, H. J., Bar, F. W., & Lie, K. I. (1978). The value of the electrocardiogram in the differential diagnosis of a tachycardia with a widened QRS complex. *The American Journal of Medicine*, *64*, 27–33.

How to cite this article: Kashou, A. H., LoCoco, S., Shaikh, P. A., Katbamna, B. B., Sehwat, O., Cooper, D. H., Sodhi, S. S., Cuculich, P. S., Gleva, M. J., Deych, E., Zhou, R., Liu, L., Deshmukh, A. J., Asirvatham, S. J., Noseworthy, P. A., DeSimone, C. V., & May, A. M. (2023). Computerized electrocardiogram data transformation enables effective algorithmic differentiation of wide QRS complex tachycardias. *Annals of Noninvasive Electrocardiology*, *28*, e13018. <https://doi.org/10.1111/anec.13018>

SUPPORTING INFORMATION

Additional supporting information can be found online in the Supporting Information section at the end of this article.